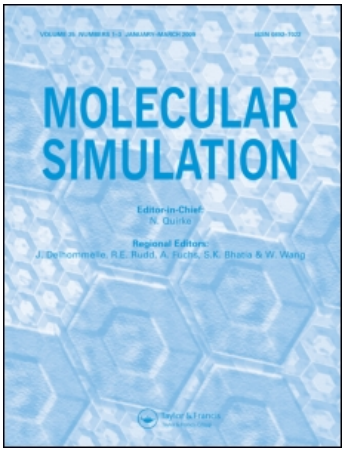

Molecular Simulation
Publication details, including instructions for authors and subscription information:
http://www.informaworld.com/smpp/title~content=t713644482

Electronic properties of graphene nanoribbons with armchair-shaped edges

S. S. Yu[a]; Q. B. Wen[a]; W. T. Zheng[a]; Q. Jiang[a]
[a] State Key Laboratory of Superhard Materials and Laboratory of Automobile Materials, MOE, Department of Materials Science, Jilin University, Changchun, People's Republic of China

To cite this Article Yu, S. S. , Wen, Q. B. , Zheng, W. T. and Jiang, Q.(2008) 'Electronic properties of graphene nanoribbons with armchair-shaped edges', Molecular Simulation, 34: 10, 1085 — 1090
To link to this Article: DOI: 10.1080/08927020801958795
URL: http://dx.doi.org/10.1080/08927020801958795

Molecular Simulation
Vol. 34, Nos. 10–15, September–December 2008, 1085–1090

Taylor & Francis
Taylor & Francis Group

Electronic properties of graphene nanoribbons with armchair-shaped edges

S.S. Yu, Q.B. Wen, W.T. Zheng* and Q. Jiang

State Key Laboratory of Superhard Materials and Laboratory of Automobile Materials, MOE, Department of Materials Science, Jilin University, Changchun, People's Republic of China

(Received 29 December 2007; final version received 1 February 2008)

Calculations based on density-functional theory are used to investigate the electronic properties of graphene nanoribbons (GNRs) with hydrogen-passivated armchair-shaped edges. It is found that their density of states (DOS) is non-symmetric, and that small splittings of some peaks of DOS occur. Also, it is confirmed that their energy band gaps depend on ribbon widths, and show a sawtooth-like shape, which is in a good agreement with others' previous results. Analysing the frontier π bonding structures and the density of electrons, we can determine that both ribbon width and edge play a key role in the electronic properties of GNRs with hydrogen-passivated armchair-shaped edges.

Keywords: graphene nanoribbon; electronic structure; density of states; armchair graphene nanoribbons

1. Introduction

Graphene nanoribbons (GNRs) are nanometer-sized graphene, in which the boundary regions play an important role [1]. Due to their structural resemblance to carbon nanotubes and due to their quantum confinement effects, GNRs are expected to present electronic properties similar to those of carbon nanotubes which can be unwrapped into GNRs [2,3]. However, some theoretical studies show that the metallic or semiconducting feature in GNRs is different from that in carbon nanotubes [1,4,5]. The electronic properties of nanoribbons are ruled by the widths and atomic geometry along the edges: namely, zigzag or armchair. Similar to armchair nanotubes, GNRs with zigzag-shaped edges are all metallic, while for GNRs with armchair-shaped edges, the band gap oscillations have been presented as a function of their width [6–8]. That is to say, GNRs can be made either as metallic or as semiconducting materials by controlling their width or chirality [9].

Several experimental groups have successfully produced 2D crystals of graphene [10–12] that are isolated and stable at room temperature. Scanning tunnelling microscopy images of graphene sheets have revealed bright stripes along their edges, suggesting a high density of edge states near the Fermi level [13,14]. Graphene is a semimetal at the micron scale or larger, but when it is trimmed down to less than 100 nm, electron confinement opens its band-gap, resulting in an effect that can be used to tune the crystal's electronics for different purposes [15]. Graphene nanoribbon has attracted enormous attention due to fundamental scientific interest in nanomaterials and due to its versatile electronic properties that are expected to be important for future application in nanoelectronics [6]. In addition, GNRs are much easier to manipulate than carbon nanotubes, and can be produced in a highly controllable manner, offering the opportunity to take advantage of the unique and well-understood electronic properties of carbon nanotubes, while circumventing the growth control problems which have been one of the major obstacles toward their wide commercial use [2].

It is well known that zigzag carbon nanotubes have special electronic properties, which depend on chiral index [16–18]. As the electronic properties of GNRs with armchair-shaped edges are similar to those of zigzag carbon nanotubes, it could be expected that GNRs with armchair-shaped edges should have similar unusual electronic properties. Some recent reports [1–3,5–7] have already described the electronic properties of GNRs with armchair-shaped edges at some specific ribbon widths and found that the energy band gaps of GNRs with armchair-shaped edges depend on the ribbon widths, but some of these investigations are based on the tight-binding approximation [1,3,7] and most of them only concentrate on the change of energy band gap with ribbon width. For low dimensional materials, the edge strain and trapping are significant because they can modify the density of states (DOS) and band gap energy [19]. Very recently, Wang et al. [20] have predicted that the chemical edge modifications can also affect the structural and electronic properties of GNRs with armchair-shaped edges. After geometry optimisation, the C—C bond length and bond angle near the edge undergo

*Corresponding author. Email: wtzheng@jlu.edu.cn

ISSN 0892-7022 print/ISSN 1029-0435 online

DOI: 10.1080/08927020801958795
http://www.informaworld.com

observable changes [20]. Under this condition, their electronic structures may be unusual compared to those of unrelaxation geometry. However, they also only concentrate themselves on the change of energy band gap, and detailed analysis of the electronic structures has not been given. Motivated by the recent experimental and theoretical progress in this area, we investigate the electronic properties of GNRs with hydrogen-passivated armchair-shaped edges in detail using density-functional theory (DFT) calculations in this work.

2. Method

The DFT package utilised for this study was Dmol3 [21,22] used through the MS MODELING ver3.1 from Accelrys Inc., (San Diego, CA, USA). In this code, each electronic wave function was expanded in a localised atom-centred basis set with each basis function defined numerically on a dense radial grid. All-electron calculations were performed with a double numeric plus polarisation basis set. For the exchange and correlation term, the generalised gradient approximation (GGA) was used as proposed by Perdew–Burke–Ernzerhof (PBE) [23]. A finite basis-set cutoff was 3.7 Å, and self-consistent-field tolerance was 1.0×10^{-6} Ha.

In order to test our method, we have calculated the DOS for perfect (10, 0) and (9, 0) zigzag single-walled carbon nanotubes. Our energy differences between the first two van Hove singularities are 0.82 eV for (10, 0) tube and 2.50 eV for (9, 0) tube, respectively. The results are in good agreement with the theoretical PBE–GGA results of Pavel et al. [24].

To mimic a situation of an isolated graphene ribbon, we adopted 3D repeating supercells in which individual ribbons are separated by a vacuum region. In the adopted vacuum region, the intervals among the ribbons were kept as 10 and 10 Å for edge–edge and layer–layer distances, respectively. These intervals were enough to ensure negligible interaction between the ribbon and its periodic image. The lengths of GNRs with armchair-shaped edges were chosen as 29.84 Å. Because of the very large supercell, only Γ sampling point in the Brillouin zone was used for geometry optimisation. C—C bond length of 1.42 Å was chosen before geometry optimisation. The geometry optimisation convergence thresholds of energy change, maximum force and displacement were 1.0×10^{-5} Ha, 0.002 Ha/Å and 0.005 Å, respectively. The positions of all the atoms including the passivated hydrogen atoms in the supercell were not constrained and could be fully relaxed under the condition that the cell parameters were fixed on the values optimised for the original supercell.

Following previous convention [1,3,5–7], the GNRs with armchair-shaped edges on both sides are classified by the number of dimer lines (N_a) across the ribbon width as shown in Figure 1. We refer to a GNR with N_a dimer lines as a N_a-AGNR (armchair graphene nanoribbon).

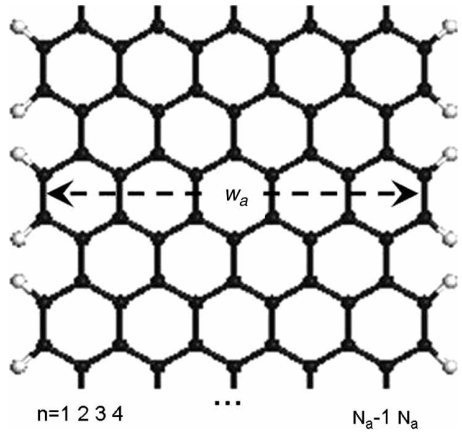

Figure 1. Schematic of a 11-AGNR. The grey balls denote hydrogen atoms passivating the edge carbon atoms, and the black balls represent carbon atoms in the graphene structure. The graphene ribbon width is represented by w_a.

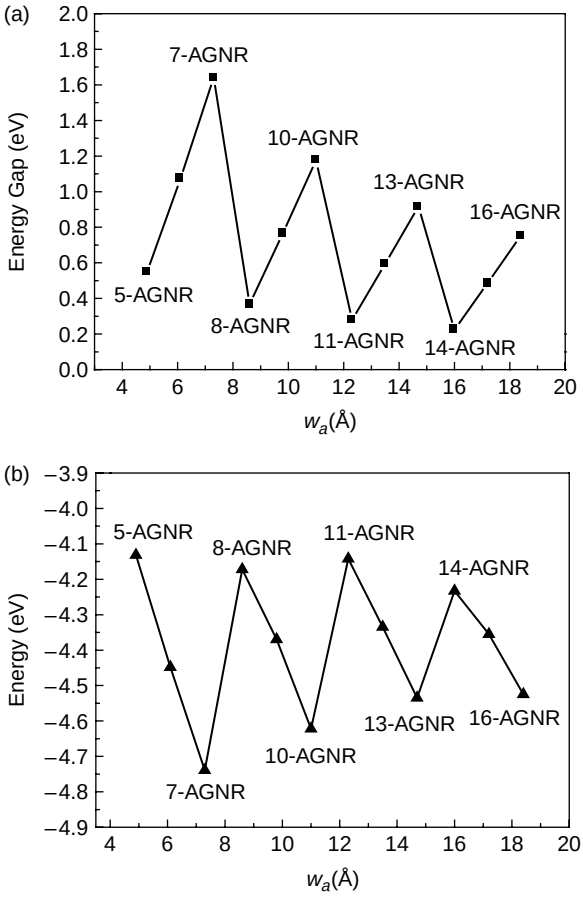

Figure 2. (a) The variation of band gaps and (b) energies of frontier π orbitals for N_a-AGNRs as a function of width (w_a).

3. Results and discussion

AGNR has a zero DOS at the Fermi level and AGNRs have a diamagnetic susceptibility [1,6]. Hence, we adopted spin-restricted DFT schemes for AGNRs. In Figure 2(a), we plot energy band gaps as a function of ribbon widths (w_a) for N_a-AGNRs with $N_a = 5–16$. The change of the band gaps with ribbon width exhibits a sawtooth-like shape, and such feature is characterised by that the band gaps of N_a-AGNRs with $N_a = 3p + 2$ (where p is a positive integer) are the lowest among three neighbouring ($N_a = 3p + 2, 3p + 1, 3p$) N_a-AGNRs, which are in good agreement with others previous results [2,6,8,9]. It is noticed that the N_a-AGNRs with $N_a = 3p + 2$ are semimetals and other N_a-AGNRs are semiconductors. These results are similar to those of corresponding zigzag carbon nanotubes [17,18]. Since the electronic properties of GNRs are mainly determined by π electrons, from Figure 2(a), we can expect that the π electrons of N_a-AGNRs with $N_a = 3p + 2$ would be more delocalised than other N_a-AGNRs. In Figure 2(b), we plot the energies of frontier π orbitals (highest occupied molecular orbital, HOMO) for N_a-AGNRs with $N_a = 5–16$. It is observed that the energies of HOMOs for the N_a-AGNRs with $N_a = 5$, 8, 11, 14, are higher than those of other neighbouring N_a-AGNRs. Consequently, for N_a-AGNRs with $N_a = 3p + 2$, the electrons that occupy the frontier π orbitals are more delocalised than other neighbouring N_a-AGNRs.

In Figure 3, we plot the nodal structures of the frontier π orbitals for the N_a-AGNRs with $N_a = 5–16$. The surfaces of constant amplitude of the wavefunctions are shown, in which the positive and negative values are denoted by dark gray and light gray nodal structures, respectively. It can be observed from Figure 3 that three different groups of the frontier π orbitals can be classified: the first one is the group with $N_a = 3p + 2$, the others are groups with $N_a = 3p + 1$ and $N_a = 3p$, respectively. It is found that, among the nodal structures of the frontier π orbitals, for N_a-AGNRs with $N_a = 3p + 2$, the closed surfaces of the wavefunctions encompass two atoms totally. In contrast, for other N_a-AGNRs, the closed surfaces of the wavefunctions encompass an additional

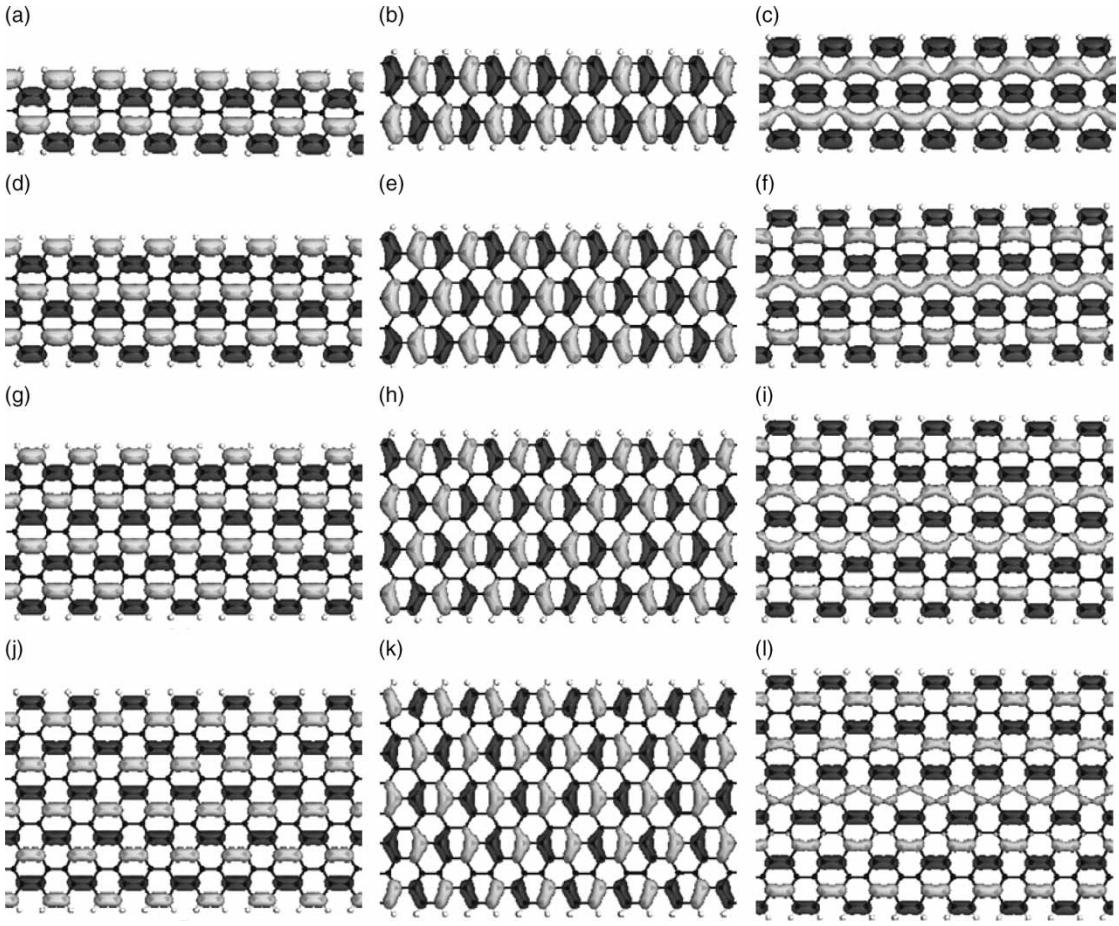

Figure 3. Qualitative description of the frontier π orbitals of N_a-AGNRs with N_a = (a) 5, (b) 6, (c) 7, ..., (k) 15 and (l) 16. The isosurface value is ± 0.012 electrons/a.u. [3] and the surfaces of constant amplitude of the wavefunctions are shown for positive values in the dark gray and for negative ones in the light gray, respectively.

atom compared with N_a-AGNRs with $N_a = 3p + 2$. Consequently, the frontier π orbital bonding structures of N_a-AGNRs with $N_a \neq 3p + 2$ are more stable than those of N_a-AGNRs with $N_a = 3p + 2$, and the energies of HOMOs for the N_a-AGNRs with $N_a = 3p + 2$ are higher than those of N_a-AGNRs with $N_a \neq 3p + 2$. However, it is found that, with the increase of ribbon width, for HOMOs of the group with $N_a \neq 3p + 2$, there appear gradually more closed surfaces of the wavefunctions encompassing two atoms near the edge. Because the quantum effects (the quantisation of wave function along ribbon width) will disappear gradually with the increase of ribbon width, the density of electrons will become small on the frontier orbitals. Therefore, the closed surfaces character on the edges that is formed by the frontier orbitals becomes weak and some closed surfaces character encompassing three or more atoms will diminish gradually. As p becomes large, for HOMOs of the group with $N_a \neq 3p + 2$, the closed surfaces of the wavefunctions will totally encompass two atoms on the edges.

The DOS of N_a-AGNRs with $N_a = 5-13$ are shown in Figure 4. It is found that all DOS are not symmetric and that small splittings of some peaks emerge. The DFT calculations of the ideal graphene should predict a set

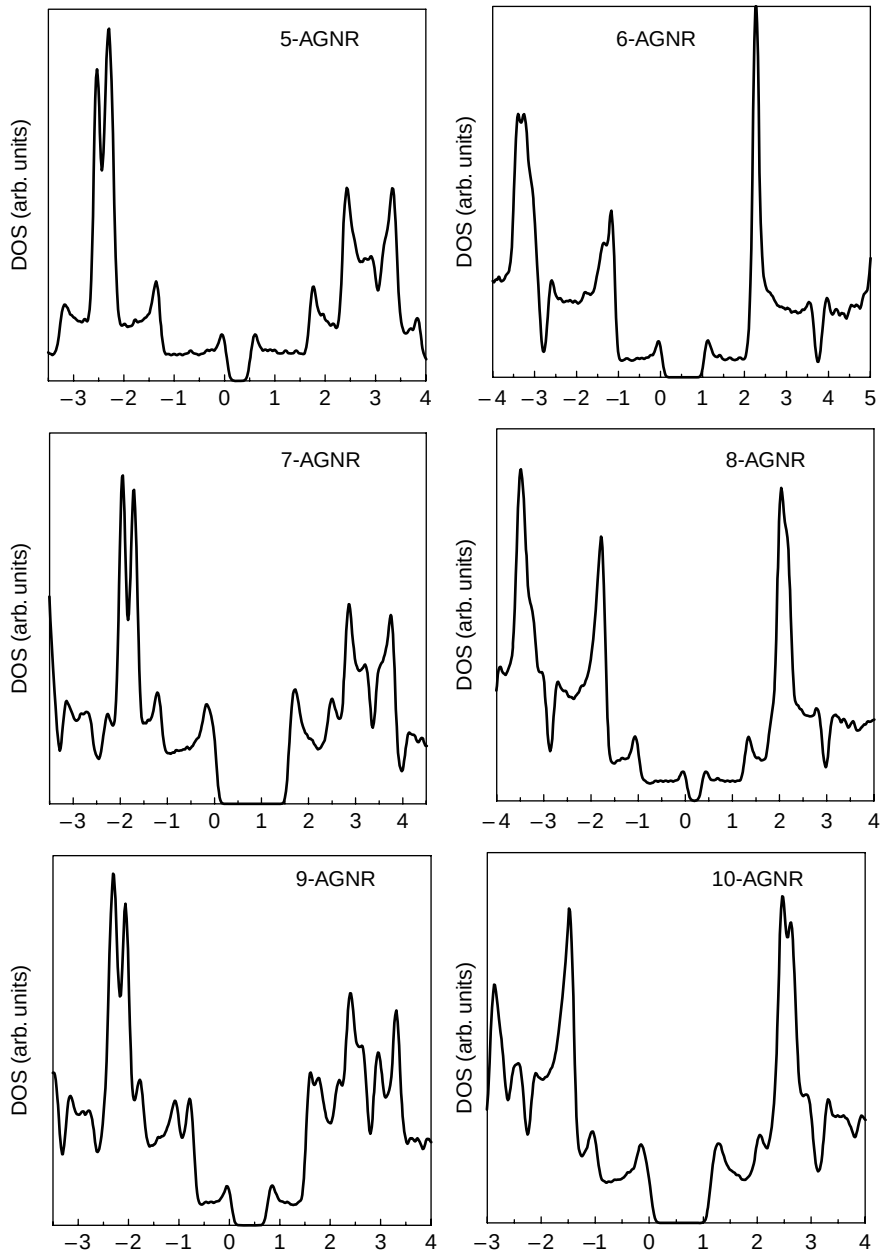

Figure 4. The DOS for the N_a-AGNRs with $N_a = 5-10$. Fermi levels are set as 0.

of equidistant levels near the Fermi level, which means that its DOS are symmetric. However, for graphene ribbon, this symmetry is broken with respect to ideal graphene, because the Fermi wave vector of the relaxed ribbon shifts smaller than Fermi level (k_F) for ideal graphene. The absolute shift is enhanced by the difference in bond lengths after relaxation. On the other hand, this anisotropy around k vector leads to that the two linear bands (π and $\pi*$) which cross the Fermi energy have different slopes [25]. As confinement of the electrons due to reduced width for graphene ribbon produces a discretisation $\Delta k = \pi/w_a$, the intersection of two linear bands (with different slopes) with Δk will result in slightly different energy dispersion $E(k)$ values, and this would account for the small splittings observed in DOS. The same phenomena also occur for single-walled carbon nanotubes with a finite size [25,26].

For AGNRs with hydrogen-passivated edges, edge effect plays an important role in electronic properties. For N_a-AGNRs with $N_a = 5-14$, the densities of electrons (DOE) of HOMOs near the edge are shown in Figure 5. We only exhibit the DOE of three rows near the edge, and their values are marked by up-triangle, circle and square, respectively. It is observed that the values of DOE become gradually smaller and smaller with increasing ribbon width and that the DOE of the second row of carbon atoms is the densest. Considering the frontier π orbital bonding structures in Figure 3, for N_a-AGNRs with $N_a = 3p + 2$, the DOE of the first and second rows are roughly equal to each other. However, for N_a-AGNRs with $N_a \neq 3p + 2$, the difference between the DOE of first and second rows becomes slighter and slighter with increasing ribbon width. Consequently, with the increase of ribbon width, the character of their DOE follows a trend similar to that of N_a-AGNRs with $N_a = 3p + 2$, which are in agreement with that in Figure 3. The frontier π orbitals of the N_a-AGNRs with $N_a \neq 3p + 2$ display less additional bonding character with the increase of ribbon width. The sums of DOE of above three rows near the edge are also exhibited in Figure 5, which are marked by filled down-triangle. It can be clearly seen that the values of DOE of the frontier π orbital bonding structures as a function of ribbon width also show a sawtooth-like shape, and such a feature can also be characterised by the lowest DOE of N_a-AGNRs with $N_a = 3p + 2$ compared to other neighbouring N_a-AGNRs. This feature is similar to that of band gap observed in Figure 2(a), which can be explained by the fact that the frontier π orbital bonding structures of N_a-AGNRs with $N_a = 3p + 2$ are weaker than those with $N_a \neq 3p + 2$. Accordingly, the electrons of N_a-AGNRs with $N_a = 3p + 2$ that occupy the frontier π orbitals are more delocalised than other N_a-AGNRs. In addition, for the group with $N_a = 3p + 1$, the values of DOE among three rows near the edge are strikingly different compared to the other two groups. Consequently, the edges have the strongest influence on the DOE of N_a-AGNRs with $N_a = 3p + 1$, and the weakest influence on that of N_a-AGNRs with $N_a = 3p + 2$. Both the quantum confinement and the edge effects are exhibited clearly in Figure 5.

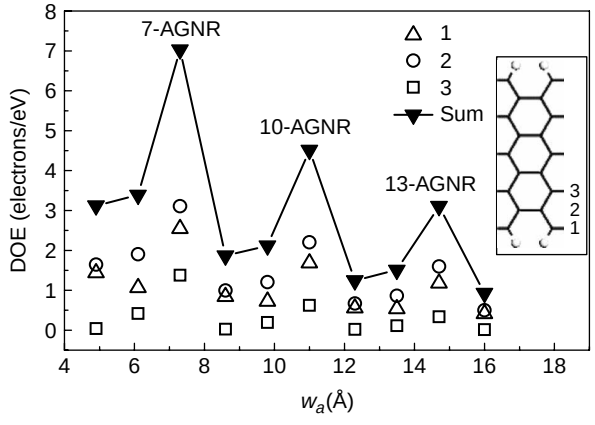

Figure 5. The density of electrons (DOE) of frontier π orbitals for N_a-AGNRs as a function of width (w_a). The DOE of the first, second and third rows near the edge and their sum are marked by up-triangle, circle, square, and filled down-triangle, respectively.

4. Conclusions

It is found that the DOS for N_a-AGNRs is non-symmetric, and two adjacent peaks in DOS emerge. Also, it is confirmed that their energy band gaps depend on ribbon widths, and show a sawtooth-like shape, which is in good agreement with other previous results. The frontier π orbitals of N_a-AGNRs with $N_a = 3p + 2$ are composed of wave functions encompassing two atoms. However, the other N_a-AGNRs acquire an additional bonding character compared with N_a-AGNRs with $N_a = 3p + 2$, with the result that the frontier π orbital bonding structures of N_a-AGNRs with $N_a \neq 3p + 2$ are more stable than that of N_a-AGNRs with $N_a = 3p + 2$. Due to the edge effect, the DOE are different among the rows in N_a-AGNRs, and the edges have the strongest influence on N_a-AGNRs with $N_a = 3p + 1$, and the weakest influence on N_a-AGNRs with $N_a = 3p + 2$. Consequently, this is a typical case of edge trapping as described by Sun [19].

Acknowledgements

Support from National Natural Science Foundation of China (Grant no. 50525204 and 50372024), the National Key Basic Research and Development Program (Grant no. 2004CB619301), Project 985 – Automotive Engineering of Jilin University, and the Teaching and Research Award Program for the Outstanding Young Teachers in High Education Institutions (Grant no. 2002359) is acknowledged.

References

[1] K. Wakabayashi, M. Fujita, H. Ajiki, and M. Sigrist, *Electronic and magnetic properties of nanographite ribbons*, Phys. Rev. B 59 (1999), pp. 8271–8282.

[2] V. Barone, O. Hod, and G.E. Scuseria, *Electron structure and stability of semiconducting graphene nanoribbons*, Nano Lett. 6 (2006), pp. 2748–2754.

[3] K. Nakada, M. Fujita, G. Dresselhaus, and M.S. Dresselhaus, *Edge state in graphene ribbons: Nanometer size effect and edge shape dependence*, Phys. Rev. B 54 (1996), pp. 17954–11760.

[4] Y.L. Lee and Y.W. Lee, *Ground state of graphite ribbons with zigzag edges*, Phys. Rev. B 66 (2002), pp. 245402-1-6.

[5] Y. Miyamoto, K. Nakada, and M. Fujita, *First-principles study of edge states of H-terminated graphitic ribbons*, Phys. Rev. B 59 (1999), pp. 9858–9861.

[6] Y.W. Son, M.L. Cohen, and S.G. Louie, *Energy gaps in graphene nanoribbons*, Phys. Rev. Lett. 97 (2006), pp. 216803-1-4.

[7] C.T. White, J. Li, D. Gunlyche, and J.W. Mintmire, *Hidden one-electron interactions in carbon nanotubes revealed in graphene nanostrips*, Nano Lett. 7 (2007), pp. 825–830.

[8] L. Brey and H.A. Fertig, *Electronic states of graphene nanoribbons studied with the Dirac equation*, Phys. Rev. B 73 (2006), pp. 235411-1-5.

[9] M. Ezawa, *Peculiar width dependence of the electronic properties of carbon nanoribbons*, Phys. Rev. B 73 (2006), pp. 045432-1-8.

[10] K.S. Novoselov, A.K. Geim, S.V. Morozov, D. Jiang, M.I. Katsnelson, V. Grigoerva, and S.V. Dubonos, *Two-dimensional gas of massless dirac fermions in graphene*, Nature 438 (2005), pp. 197–200.

[11] Y.B. Zhang, Y.W. Tan, H.L. Stormer, and P. Kim, *Experimental observation of the quantum Hall effect and Berry's phase in graphene*, Nature 438 (2005), pp. 201–204.

[12] S. Stankovich, D.A. Dikin, G.H.B. Dommett, K.M. Kohlhaas, E.J. Zimney, E.A. Stach, R.D. Piner, S.T. Nguyen, and R.S. Ruoff, *Graphene-based composite materials*, Nature 442 (2006), pp. 282–286.

[13] Y. Niimi, T. Matsui, H. Kambara, K. Tagami, M. Tsukada, and H. Fukuyama, *Scanning tunneling microscopy and spectroscopy of the electronic local density of states of graphite surfaces near monoatomic step edges*, Phys. Rev. B 73 (2006), pp. 085421-1-8.

[14] Y. Kobayashi, K.I. Fukui, T. Enoki, and K. Kusakabe, *Edge state on hydrogen-terminated graphite edges investigated by scanning tunneling microscopy*, Phys. Rev. B 73 (2006), pp. 125415-1-8.

[15] M. Wilson, *Electrons in atomically thin carbon sheets behave like massless particles*, Phys.Today 59 (2006), pp. 21–23.

[16] N. Hamada, S.I. Sawada, and A. Oshiyama, *New one-dimensional conductors: Graphitic microtubules*, Phys. Rev. Lett. 68 (1992), pp. 1579–1581.

[17] S.S. Yu, W.T. Zheng, Q.B. Wen, B. Zheng, H.W. Tian, and Q. Jiang, *Nature of substitutional impurity atom B/N in zigzag single-wall carbon nanotubes revealed by first-principle calculations*, IEEE Trans. Nanotechnol. 5 (2006), pp. 595–598.

[18] S.S. Yu, Q.B. Wen, W.T. Zheng, and Q. Jiang, *Effects of doping nitrogen atoms on the structure and electronic properties of zigzag single-walled carbon nanotubes through first-principles calculations*, Nanotechnology 18 (2007), pp. 165702-1-7.

[19] C.Q. Sun, *Size dependence of nanostructures: Impact of bond order deficiency*, Prog. Solid State Chem. 35 (2007), pp. 1–159.

[20] Z.F. Wang, Q.X. Li, H.X. Zheng, H. Ren, H.B. Su, Q.W. Shi, and J. Chen, *Tuning the electronic structure of graphene nanoribbons through chemical edge modification: A theoretical study*, Phys. Rev. B 75 (2007), pp. 113406-1-4.

[21] B. Delley, *An all-electron numerical method for solving the local density functional for polyatomic molecules*, J. Chem. Phys. 92 (1990), pp. 508–517.

[22] B. Delley, *From molecules to solids with the Dmol3 approach*, J. Chem. Phys. 113 (2000), pp. 7756–7764.

[23] J.P. Perdew, K. Burke, and M. Ernzerhof, *Generalized gradient approximation made simple*, Phys. Rev. Lett. 77 (1996), pp. 3865–3868.

[24] A.V. Pavel, K.N. Konstantin, and S.E. Gustavo, *Single wall carbon nanotubes density of states: Comparison of experiment and theory*, Chem. Phys. Lett. 370 (2003), pp. 597–601.

[25] A. Rubio, D. Sanchez-Portal, E. Artacho, P. Ordejon, and J.M. Soler, *Electronic states in a finite carbon nanotube: A one-dimensional quantum box*, Phys. Rev. Lett. 82 (1999), pp. 3520–3523.

[26] T.W. Odom, J. Huang, P. Kim, and C.M. Lieber, *Structure and electronic properties of carbon nanotubes*, J. Phys. Chem. B 104 (2000), pp. 2794–2809.